This is a repository copy of *Online pricing for demand-side management in a low-voltage resistive micro-grid via a Stackelberg game with incentive strategies*.

White Rose Research Online URL for this paper:
https://eprints.whiterose.ac.uk/178568/

Version: Published Version

Article:
Genis Mendoza, F. orcid.org/0000-0001-7483-0654, Konstantopoulos, G. orcid.org/0000-0003-3339-6921 and Bauso, D. (2022) Online pricing for demand-side management in a low-voltage resistive micro-grid via a Stackelberg game with incentive strategies. IET Smart Grid, 5 (2). pp. 76-89. ISSN 2515-2947

https://doi.org/10.1049/stg2.12053

Reuse
This article is distributed under the terms of the Creative Commons Attribution (CC BY) licence. This licence allows you to distribute, remix, tweak, and build upon the work, even commercially, as long as you credit the authors for the original work. More information and the full terms of the licence here: https://creativecommons.org/licenses/

Takedown
If you consider content in White Rose Research Online to be in breach of UK law, please notify us by emailing eprints@whiterose.ac.uk including the URL of the record and the reason for the withdrawal request.

eprints@whiterose.ac.uk
https://eprints.whiterose.ac.uk/

Received: 24 June 2021 | Revised: 19 August 2021 | Accepted: 29 August 2021

IET Smart Grid

DOI: 10.1049/stg2.12053

The Institution of Engineering and Technology WILEY

ORIGINAL RESEARCH PAPER

Online pricing for demand-side management in a low-voltage resistive micro-grid via a Stackelberg game with incentive strategies

Fernando Genis Mendoza[1] | **George Konstantopoulos**[1,2] | **Dario Bauso**[3,4]

[1]Department of Automatic Control and Systems Engineering, The University of Sheffield, Sheffield, UK

[2]Department of Electrical and Computer Engineering, University of Patras, Rion, Greece

[3]Jan C. Willems Center for Systems and Control ENTEG, Faculty of Science and Engineering, University of Groningen, Groningen, The Netherlands

[4]Dipartimento di Ingegneria, Università di Palermo, Palermo, Italy

Correspondence

Fernando Genis Mendoza, Department of Automatic Control and Systems Engineering, The University of Sheffield, Mappin Street, Sheffield, S1 3JD, UK.
Email: fgenismendoza1@sheffield.ac.uk

Funding information

Engineering and Physical Sciences Research Council, Grant/Award Numbers: EP/S001107/1, EP/S031863/1; C. CARATHEODORY Program: 81359

Abstract

It has been demonstrated that online pricing mechanisms are a viable solution for demand side management in power systems. This study deals with the analysis and design of a droop-controlled low-voltage resistive AC micro-grid network system. Such a system is subjected to a dynamic demand obtained from an online pricing mechanism, which is proposed as a novelty in the study of micro-grids. This mechanism is derived from a variation of the Stackelberg game, which includes the use of incentive strategies. First, a configuration in which a supplier announces an incentive function and n-consumers' reaction to the resulting personalised price is presented. Then, a detailed stability analysis of the micro-grid is presented as a result of the interaction with the aforementioned online pricing mechanism. The units of the micro-grid (generators as the supplier and loads as the consumers) operate under either conventional or bounded droop control. The novelty of the approach is that it bridges the gap between the physical and the market layers of the problem. The ways in which the existence of multiple equilibrium points is guaranteed for both the consumer's load and the supplier's announced incentive are shown. A detailed design process for the profit functions of the players is shown in conjunction with the parameter selection for their implementation. Finally, simulations that demonstrate the system stability and its convergence to different equilibria are implemented under scenarios with one and multiple consumers.

1 | INTRODUCTION

In electrical power systems, the implementation of real-time pricing mechanisms represents a viable way to shift demand during peak times, thus improving efficiency without compromising the functioning of the generation and distribution systems themselves. The general purpose of these mechanisms is to facilitate the supplier means to charge more when the generation costs are higher, and conversely, to let the consumer know when the price has decreased and it is more convenient to carry out more power-demanding tasks. The underlying assumption is that both the consumers and the suppliers are rational agents and have the objective of maximising their profits. Under such an assumption, a change in price results in a change of consumption. The implementation of effective dynamic pricing methods remains an open problem and introduces challenges such as global optimality for both suppliers and consumers, uncertainties in their behaviours and preferences, and more importantly, safe operation of the electrical systems when subjected to such methods. This last issue is the main motivation of this work; as we will reiterate later, most literature about dynamic pricing does not focus on the analysis of the impact on stability when implementing such mechanisms onto a realistic physical electrical system. Furthermore, since the game-theoretic Stackelberg approach has been proposed for this kind of systems before, we differentiate our work by introducing the concept of

This is an open access article under the terms of the Creative Commons Attribution License, which permits use, distribution and reproduction in any medium, provided the original work is properly cited.

© 2021 The Authors. *IET Smart Grid* published by John Wiley & Sons Ltd on behalf of The Institution of Engineering and Technology.

incentive strategies, which briefly explained, allow the inclusion of *offers* and other functions for the price into the pricing scheme.

1.1 | Problem statement

The focus of this study consists in providing a clear insight into the interaction between the physical and market dynamics of the online pricing problem. The main purpose is to obtain a better understanding of how to implement such a mechanism and how to predict its impact on the physical system. This is achieved by performing an analysis of an industrial low-voltage resistive micro-grid system, where both the generators and the loads are in the grid-forming mode (droop controlled units), as required in modern power systems, and the load demand is subject to a pricing mechanism from the corresponding leader–follower market structure. We propose and adopt a Stackelberg approach with incentive strategies and a related closed-loop configuration that enables the implementation. However, a detailed analysis for both the system stability and the game operation is necessary to obtain the conditions that ensure the correct operation of the whole integrated system.

1.2 | Main contributions

As a first result, we propose a novel pricing mechanism, novel in micro-grid literature, which is based on a Stackelberg game involving incentive strategies. A characterisation of the equilibrium points is derived. Secondly, we present the conditions for stability of the resistive micro-grid model. The underlying assumption is that every generator and (industrial) load is interfaced with the micro-grid through a power inverter that operates under the P-V droop control (resistive droop), and the loads receive a power reference value given by a pricing scheme. The implementation of the proposed scheme is further simplified by adopting a P-V bounded droop controller. Numerical implementations are carried out, where the strategic competition between the consumer and the follower is shown. Convergence to different equilibrium points for different incentive strategies is also illustrated. A way in which the parameters can be selected for its application is likewise delineated.

1.3 | Reviewed literature

This study is an extension of the study in [1], where we proposed a normalised game for a single AC micro-grid. The formulation for the supplier and consumer models used here is introduced in [2] and used also in [3]. The fundamental theoretical concepts for the Stackelberg game are explained in [4], while the variation of such games with the inclusion and formulation of the incentive strategy was originally introduced in [5]. Examples of the use of the Stackelberg equilibrium for demand management problems are found in [6–10] and [11], where [6, 7] focus mainly on electric vehicle charge management and [8] demonstrates its feasibility numerically. The existence of equilibrium points using game theoretic approaches including the Stackelberg equilibrium is demonstrated in [9, 10]; in [11] the Stackelberg approach is used in conjunction with evolutionary algorithms for online pricing schemes. The use of incentives on micro-grids has been previously studied in [3] and, opposed to the work presented, is implemented as a reward to the consumer for participating in an online pricing scheme.

Regarding the physical plant, the resistive micro-grid network dynamics are introduced and analysed in [12, 13], the derivation of the system's conductance matrix in [14], and its characteristics and interpretation as a loopy Laplacian matrix is explained in [15]. Such dynamics are subjected to a quadratic droop control in [16].

The approximation of the demand response as a first-order dynamics is introduced in [17]; examples of this for households and businesses can be found in [18–20]. A cost function for electricity generation is presented in [21], which is used regularly in the literature, such as in [3]. A formulation for the price of energy as a proportional function of the total demand from all the users is also proposed in [21]; other examples of this practice are found in [22, 23]. For the sake of practicality, the linear price function and generation cost function used here have been based and adopted on the ones from [17].

Although the use of the Stackelberg equilibrium in demand-side management for micro-grids is already in the literature [6–11], to the best of our knowledge, the majority of studies that make use of it do not take into account the stability of the physical systems where such schemes are applied [6–11].

The key novelties of the proposed methodology compared to the existing literature are (i) the extension of the analysis in [1] to a more realistic model of a low-voltage resistive network system, (ii) the direct calculation of the steady-state gain for the consumer response in the game by employing the derived profit function, and this represents a novelty if compared to [1], (iii) different from [6–11], the inclusion of the incentive strategy as a means for a personalised price function, (iv) the integration of the electrical system, which integrates a droop-control dynamic structure for each unit with the game-theoretical part of the problem, and (v) the stability analysis of the system including an extension for the case with the bounded droop control [24, 25], which leads to simplified stability conditions.

According to the authors' knowledge, this is the first time that a droop-controlled resistive micro-grid is subjected directly to a game-theoretic pricing scheme, thus paving the way for the application of game theory-based intelligent demand-side management in future distribution systems.

1.4 | Notation preliminaries

Given the one-dimensional vector $x \in \mathbb{R}^n$ with individual elements $x_i \in \mathbb{R}$, where $i = 1, 2, \ldots, n$, we denote

$[x] = diag(x) = diag(x_i) \in \mathbb{R}^{n\times n}$ as the associated square diagonal matrix with the elements of vector x in the diagonal entries. Let us review the property $[x]^{-1} = [x_i^{-1}]$. Let $\mathbf{0}_{n\times n}$ denote a $n \times n$ matrix with all entries equal to zero and $\mathbf{1}_{n\times 1}$ be a column vector of n elements with all entries equal to one.

2 | MICRO-GRID MODEL

In this section, we introduce the dynamic models of both the micro-grid network and the droop controlled units (generators and loads).

2.1 | Network modelling review

The topology of our micro-grid network is represented by a connected, undirected and weighted graph $\mathcal{G}(\mathcal{V}, \mathcal{E})$, where $\mathcal{V} = \{1, 2, \ldots, n\}$ is the set of nodes (vertices). We divide the set of nodes in loads $\mathcal{V}_L = \{1, 2, \ldots, l\}$ and generators $\mathcal{V}_G = \{l+1, l+2, \ldots, n\}$, where $\mathcal{V} = \mathcal{V}_G \cup \mathcal{V}_L$, l is the number of load nodes and n is the total number of nodes. The set of edges $\mathcal{E} \subseteq \mathcal{V} \times \mathcal{V}$ is the set of unordered pairs $\{i, j\}$ in consideration of the distribution lines, which are assumed to be resistive. Let $A \in \mathbb{R}^{n\times n}$ denote the adjacency matrix of graph $\mathcal{G}$, where its ijth element A_{ij} is the corresponding edge represented by a conductance $1/R_{ij}$ between nodes i and j. The set $\mathcal{N}_i$ refers to the neighbouring nodes j of node i, where $\mathcal{N}_i \in \mathcal{V} : \{i, j\} \in \mathcal{E}$.

2.2 | Resistive micro-grid model

The micro-grid model under consideration has a low-voltage configuration, also known as a resistive micro-grid. The system is considered as a network of load nodes and generator nodes as shown in Figure 1, where the supplier is considered to be the owner of such generators and each consumer is represented by a load node. Note that the main grid is considered as a generator. The network is assumed to be resistive, namely the impedance of the line, which is usually resistive-inductive and is dominated by the resistive component; hence the reactive power is neglected [12].

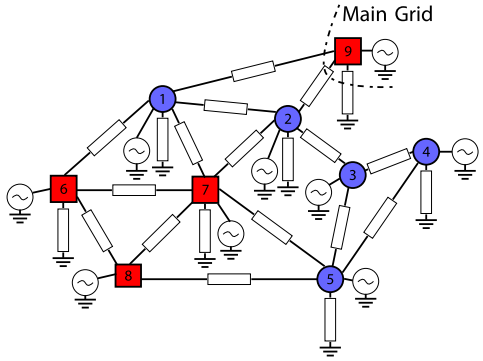

FIGURE 1 Resistive micro-grid in a network representation, comprising loads (blue circles) and generators (red squares), resistive distribution lines, and shunt conductances

The micro-grid is considered to be connected to the main grid that contributes power when the demand is higher than the supply provided by the generators; in the network topology, the main grid is considered as an additional node. However, the results explained here also apply for the case when the micro-grid is islanded.

The power equation of a node i, as a function of its adjacent nodes' voltages in a resistive micro-grid is given by

$$P_i = V_i^2\left(\frac{1}{R_{ii}} + \sum_{j\in\mathcal{N}_i}\frac{1}{R_{ij}}\right) - \sum_{j\in\mathcal{N}_i}\frac{V_iV_j}{R_{ij}}\cos\phi_{ij}, \qquad (1)$$

where V_i is the voltage on node i, P_i is the node power, R_{ij} is the resistance of the line that connects nodes i and j, R_{ii} is the shunt resistance of node i, and ϕ_{ij} is the phase difference between nodes i and j. Assuming standard decoupling approximation [3, 16], namely that the phase ϕ_{ij} has values near to zero, we obtain for the node power P_i the following non-linear expression:

$$P_i = V_i^2\left(\frac{1}{R_{ii}} + \sum_{j\in\mathcal{N}_i}\frac{1}{R_{ij}}\right) - \sum_{j\in\mathcal{N}_i}\frac{V_iV_j}{R_{ij}}. \qquad (2)$$

The power of all the nodes of the network is given by the following non-linear expression:

$$P = [V]GV, \qquad (3)$$

where P and V are vectors containing all the nodes' powers and voltages, respectively, and G is the conductance matrix [14] that is derived from the network's Laplacian. Let us briefly explain some of the properties of G in the next subsection.

2.3 | Definition and properties of the conductance matrix

Let A denote the adjacency matrix of the micro-grid network. The degree matrix of A is defined as $D := [\{\sum_{j=1}^{n} A_{ij}\}_{i=1}^{n}]$, while the Laplacian L of A is obtained as $L := D - A$. Note that, although apparent in A, the self-loops in the topology represented by the shunt conductances $A_{ii} = 1/R_{ii} = g_i$ do not appear in L. For this reason, we recur to the conductance matrix G, which has the form of a loopy Laplacian matrix [15] and is defined as $G := L + [\{A_{ii}\}_{i=1}^{n}]$. The conductance matrix G has the following properties: its ijth element $g_{ij} = -1/R_{ij}$ and its diagonal elements $g_{ii} = 1/R_{ii} + \sum_{j\in\mathcal{N}_i} 1/R_{ij} = g_i - \sum_{j\in\mathcal{N}_i} g_{ij}$. If there is no connection between two nodes i and j, namely $j \notin \mathcal{N}_i$, then $g_{ij} = 0$. If node i does not contain a shunt conductance, then $g_i = 0$. Note that G as a loopy Laplacian

matrix [15], makes the system dynamics (3) resemble a nonlinear consensus dynamics [26].

2.4 | Additional model conventions

It is important to mention that the power injection P_i is positive for generators and negative for loads. The node sequence in the proposed network topology consists of the loads first and then the generators and the main grid, yielding a voltage vector $V = [V_1, V_2, \ldots, V_l, V_{l+1}, V_{l+2}, \ldots, V_n]^T$, where l is the number of loads in the network, and the nth node corresponds to the main grid. We denote the power contributed by the main grid that the network is connected to as $P_{mg} = P_n$.

2.5 | P-V droop controller

Following the architecture of modern smart grids [27], it is considered that the micro-grid is dominated by inverter- and rectifier-interfaced units, that is, both generators and loads, operating under the droop control concept to support the grid. Due to the resistive nature of low-voltage AC micro-grids, the P-V droop controller should be adopted [28]; hence, the voltage dynamics for every node take the following form:

$$\tau_v \dot{V} = (V^* \mathbf{1}_{n\times 1} - V) - k(P - P^{set}), \tag{4}$$

where $\tau_v = diag(\tau_{vi})$ and $k = diag(k_i)$ are diagonal matrices containing all the nodes' voltage time constants and power droop coefficients, respectively, V^* is the rated voltage value and P^{set} is a vector representation of the reference power either demanded or generated that is set for each node by a supervisory controller.

The vector P^{set} contains consumption rated values P_i^{Lrated}, $\forall i \in \mathcal{V}_L$. For configurations where the main grid is included, $P_{mg}^{set} = P_{mg}^{Lrated} = 0$ in order to supply any additional demand to the micro-grid or absorb any excess generation. For practicality and for generalisation, we are including such nodes for the remainder of this manuscript. Substituting (3) in (4), we obtain the dynamics for the resistive network as follows:

$$\dot{V} = -\tau_v^{-1} V - k\tau_v^{-1}[V]GV + \tau_v^{-1} V^* \mathbf{1}_{n\times 1} + k\tau_v^{-1} P^{set}. \tag{5}$$

Now we are ready to state our problem formulation.

3 | PROBLEM FORMULATION

We will incorporate a novel Stackelberg pricing scheme in the field of micro-grids where we consider the existence of a supplier of electricity and l-consumers. The supplier can be represented by a distribution network operator (DNO) or an independent system operator (ISO) that possesses a distributed set of generators. The set of consumers are represented by the controllable responsive load nodes included in (5). The generators take various P^{set} values, obtained by a supervisory controller or a maximum power point tracking algorithm that concurrently generate different costs to the supplier, triggering a change of price. As a consequence, this shifts the demand in the consumer load. Such a change of P^{set} in the supplier's generators exemplifies a variation of the power outputted by renewable resources.

Both suppliers and consumers are modelled to be price-taking, profit-maximising agents [2, 3]. We refer to *profit* in monetary terms as the remainder of the earnings minus the costs of generating/consuming power. In order to maximise their profit, the supplier wants to use a price as large as possible and the consumers want to consume as much as they can afford at the announced price. The output of the supplier is the price Λ, which is determined by a function $\Gamma(\cdot)$ called an *incentive strategy*, and the output of the consumer is a shift on consumption D_i^{set}. These are selected as the quantities that maximise their profit functions Π_S and Π_C, respectively [2].

We have now defined both the pricing scheme and the micro-grid network dynamics (5). We will use the announced price and the decided demand to obtain the stability conditions for the integrated system in a closed-loop configuration; this includes the droop control, load dynamics, and the tension between the supplier and consumers.

4 | MAIN RESULTS

In this section, first we make a brief introduction to the pricing mechanism and explain our proposed variation. Second, we explain how the physical model is subjected to the outcome of the price change and obtain the conditions for stability. Third, we formulate in detail the equations involved and demonstrate the existence and expression for the resulting equilibrium points. Finally, we show the influence of such equilibrium points on the dynamics of the physical system.

4.1 | Consumer and supplier functions

Having described the physical dynamics and the problem formulation, let us continue with the game theoretical part of our problem. For the sake of brevity and with some abuse of notation, let us denote the game and the ways in which outputs Λ and D_i^{set} are calculated as

$$\begin{aligned} \Lambda = \Gamma(\cdot) &= \arg\max_{\Gamma} \ \Pi_S(\Gamma), \\ &= \arg\max_{\Gamma} \ \Lambda P_S - c(\Gamma), \end{aligned} \tag{6}$$

for the supplier and

$$\begin{aligned} D_i^{set} &= \arg\max_{D_i^{set}} \ \Pi_C(D_i^{set}), \\ &= \arg\max_{D_i^{set}} \ v(D_i^{set}) - \Lambda P_C, \ \forall i \in \mathcal{V}_G \end{aligned} \tag{7}$$

for each consumer, where P_S is the total power supplied by the supplier, namely $P_S = \sum_{i\in\mathcal{V}_G} P_i$ and P_C is the power consumed by a consumer i, that is, $P_C = P_i^{Lrated} + D_i^{set},\ \forall i \in \mathcal{V}_L$. The earnings of the supplier is denoted by the product ΛP_S and the money paid by the consumer as ΛP_C. The value function of a consumer in the grid is denoted by $v(\cdot)$, which represents the value obtained by utilising a quantity of electricity. Analogously, the supplier has a production cost function $c(\cdot)$. We assume that such values and cost functions monotonically increase and are concave and convex, respectively [2, 3]. The inclusion of both simultaneous maximisation problems motivates the use of game-theoretical concepts such as the Stackelberg game equilibrium, which we will analyse whilst we fully formulate the profit functions of the game in the following section.

4.2 | Stackelberg game formulation

The Stackelberg game refers to a hierarchical structure, according to which there is a leader and there are followers (in our case a supplier and consumers, respectively). Our system set-up accommodates such structures where the leader plays first, and the output of the consumer depends on the announced output of the supplier. The supplier in turn has selected its output as the best one from a set.

Unlike in a standard Stackelberg game, setting the output of the leader to be a function enables the existence of multiple equilibrium points [1, 5]. This allows the follower to decide an output that aligns with its necessities. This is the main advantage of this variation of the game, where instead of a unique equilibrium point, the follower can select its best response from the multiple options yielded by the announced incentive—all while the game is at an equilibrium.

For the sake of tractability, let us define the incentive strategy $\Gamma(\cdot)$ based on the following assumption, although without loss of generality, other types of strategies/functions can be selected in a similar manner.

Assumption 1 The incentive strategy $\Gamma(\cdot)$ is a linear function and is given by

$$\Gamma(P_i^L) \coloneqq \Lambda_i = \gamma P_i^L, \tag{8}$$

where γ is a positive scalar gain. The endogenous variable P_i^L is the power consumed by load i that is being measured before the game is played.

The above can be interpreted as a function for a *personalised* price Λ_i that depends on how much power each consumer is using. In simpler terms, the aforementioned strategy can represent an *offer* that *incentivises* consumption, where the offer can take the form of the proposed $\Gamma(\cdot)$ function. This is a sensible assumption, since the price would be calculated proportionally to the demand, in the same spirit as in the literature about demand management [21], incentive strategies [1, 22], and dynamic pricing [23].

The gain γ is defined as strictly positive in our set-up since a negative value would represent the supplier paying the consumer. For consistency and for the remainder of this study we will refer to γ as the *incentive value*.

Let us introduce the quantity P_G, which is the total power supplied by the supplier's generators in the network. This does not include the main grid in node n, namely $P_G = \sum_{i\in\mathcal{V}_G\setminus n} P_i$. The power lost in the distribution lines of the network P_{loss} is the remainder of all the power generated minus the sum of measured powers on the nodes. This is calculated as $P_{loss} = \sum_{i\in\mathcal{V}_G} P_i - |\sum_{i\in\mathcal{V}_L} P_i|$.

Remark 1 For the sake of simplicity, we use the above expression to obtain a measure of the power losses. However, the power loss can also be calculated as $P_{loss} = \sum_{i\in\mathcal{V}_G} V_i^2 g_{ii}$; we avoid the use of such an expression since it involves the system's state vector.

As mentioned in Section 4.1, from (8), the money paid by the consumer i is rewritten as $\gamma P_i^L (D_i^{set} + P_i^{Lrated})$ and the earnings of the supplier as $\gamma \sum_{i\in\mathcal{V}_L} (P_i^L)^2$; both quantities are equal to the price times the respective power consumption/supply. The remaining elements of (6) and (7) are explained as follows: We define both cost and value functions of the supplier and consumers, respectively, as

$$\begin{aligned} c(\cdot) \coloneqq c(\gamma, P_G, P_{mg}, P_{loss}) = \alpha_G (\gamma P_G)^2 + \alpha_G (\gamma P_{loss})^2 \\ + \alpha_{mg} (\gamma P_{mg})^2, \end{aligned} \tag{9}$$

$$v(\cdot) \coloneqq v(D_i^{set}) = \alpha_{Ci} \ln(P_i^{Lrated} + D_i^{set}), \tag{10}$$

where it is clear that $c(\cdot)$ and $v(\cdot)$ are convex and concave, respectively, α_G is a scalar gain directly associated with the cost of running/operating the supplier's own network generators, and α_{mg} is associated with the cost of borrowing power from the main grid. Both positive scalars are selected and derived exogenously according to various factors such as market conditions, time of the year etc. Analogously, α_{Ci} represents each consumer's own preference for consuming power. As their names suggest, the cost and value functions represent monetary quantities for the players and the above gains are used to also adjust such functions' units. All of the above yields the maximisation problems and profit functions now rewritten as

$$\begin{aligned} &\arg\max_{\gamma} \ \gamma \sum_{i\in\mathcal{V}_L} (P_i^L)^2 - c(\gamma, P_G, P_{mg}, P_{loss}), \\ &\arg\max_{D_i^{set}} \ v(D_i^{set}) - \gamma P_i^L (D_i^{set} + P_i^{Lrated}),\ \forall i \in \mathcal{V}_L \end{aligned} \tag{11}$$

for the supplier and each of the consumers, respectively, where the supplier computes and announces an incentive γ that results in l output prices Λ_i. Based on this, the consumers calculate a power shift D_i^{set}. The characterisation of a Stackelberg equilibrium for the game (11) is established in the following:

Theorem 1 *Let Assumption 1 hold and consider the cost and value functions (9)–(10) in the maximisation problem (11). The Stackelberg game yields the following equilibrium points as functions of γ:*

$$\Lambda_i^* = \gamma P_i^L, \tag{12}$$

$$D_i^{set*} = \frac{\alpha_{Ci}}{\gamma P_i^L} - P_i^{Lrated}. \tag{13}$$

Proof Due to the concavity of (10), the follower's maximum is obtained by taking the derivative of Π_C in (11) and setting it equal to zero,

$$\frac{\partial \Pi_C}{\partial D_i^{set}} = \alpha_{Ci} \frac{1}{D_i^{set} + P_i^{Lrated}} - \gamma P_i^L = 0. \tag{14}$$

The derivative (14) yields a function of both player outputs as in a standard Stackelberg game, from (8), and solving for D_i^{set} in (14) yields the conditions in (12)–(13). □

The game is played every determined period of time T_S. The resulting D_i^{set} from the maximisation problems (11) is then filtered through the first-order system (15), feeding back the consumptions as will be explained in Section 4.3.

Now that the pricing mechanism has been defined, emphasis will be given to establishing the stability conditions for the physical system, where the input is the shift in consumption D_i^{set} from above.

4.3 | Closed-loop configuration

After each consumer i has decided how much to shift its consumption, namely all D_i^{set} values for each load node have been outputted by the game, these are reflected in the microgrid system by feeding them back into it. Although a decision of how much power a load should be consuming is taken at every time step when a price is announced, the load introduces a dynamic response. This is captured by a first-order dynamics as follows:

$$\tau_i \Delta \dot{P}_i^L = D_i^{set} - \Delta P_i^L, \forall i \in \mathcal{V}_L, \tag{15}$$

where $\tau_i \in \mathbb{R}_{>0}$ is the time constant of the system and ΔP_i^L is our new consumption shift state. This represents the consumers' response while they shift their consumption before reaching their selected value D_i^{set} [1, 17]. From (15), it is straightforward to show that at steady-state $\Delta P_i^{L^{ss}} = D_i^{set}$. A similar demand response modelling is often found in the literature, such as in [18, 19].

The way in which our system is subjected to the price change results from integrating the dynamics (5)–(15). This yields a state vector with the form $[V_1, \ldots, V_n, \Delta P_1^L, \ldots, \Delta P_l^L]^T$. The added states ΔP_i^L are subtracted to their respective load node powers in the vector P^{set} in (5), yielding $P_i^{set} = P_i^{Lrated} - \Delta P_i^L$ if $i \in \mathcal{V}_L$. In other words, the resulting shift of demand given a new price is reflected by modifying the rated load values. For each of the load nodes, dynamics (5) are now modified as follows:

$$\begin{aligned} \dot{V}_i = &-\frac{1}{\tau_{vi}} V_i - \frac{k_i}{\tau_{vi}} V_i^2 g_{ii} - \frac{k_i}{\tau_{vi}} V_i \sum_{j \in \mathcal{N}_i} V_j g_{ij} \\ &+ \frac{k_i}{\tau_{vi}} (P_i^{Lrated} - \Delta P_i^L) + \frac{1}{\tau_{vi}} V_i^*, \forall i \in \mathcal{V}_L. \end{aligned} \tag{16}$$

For the rest of the nodes, namely the generator nodes and the main grid node, their dynamics are left unchanged as in (5). For the sake of completeness, let us write their dynamics as

$$\begin{aligned} \dot{V}_i = &-\frac{1}{\tau_{vi}} V_i - \frac{k_i}{\tau_{vi}} V_i^2 g_{ii} - \frac{k_i}{\tau_{vi}} V_i \sum_{j \in \mathcal{N}_i} V_j g_{ij} \\ &+ \frac{k_i}{\tau_{vi}} P_i^{set} + \frac{1}{\tau_{vi}} V_i^*, \forall i \in \mathcal{V}_G. \end{aligned} \tag{17}$$

Now that we have the full dynamics of the system subject to the change of demand due to an announced price, we can perform a stability analysis.

4.4 | Closed-loop stability

Due to the non-linear nature of (15)–(17), in the sequel, we recur to the method of linearising around an equilibrium. This provides local stability results.

Calculating the Jacobian of (15)–(17), we analyse the system under the assumption of the existence of an equilibrium point; we follow the methodology for resistive networks as in [16] and references therein. We also resort to [29], Theorem 1], which states that a non-linear circuit system is to be studied near the equilibrium via linearisation for $V \in \mathbb{R}_{>0}$; this is true for our case.

Assumption 2 For constant inputs D_i^{set} $\forall i \in \mathcal{V}_L$ and P_i^{set} $\forall i \in \mathcal{V}_G$ with $P_{mg}^{set} = 0$, there exists an equilibrium point $[\bar{V}_1, \ldots, \bar{V}_n, \Delta \bar{P}_1^L, \ldots, \Delta \bar{P}_l^L]^T$ for system (15)–(17), where $\bar{V}_i \in \mathbb{R}_{>0}$ and $\Delta \bar{P}_i^L \in \mathbb{R}$.

Although the droop control model is standard, the above assumption might seem conservative. We utilise it for simplicity as a means to approximate the position of the system eigenvalues. This assumption is relaxed in Section 4.5, Assumption 3. We should mention that in a practical scenario, the droop controller has to be designed in a way such that it outputs positive voltage values [30, 31]. Additionally, the fact that the output voltages are at an equilibrium other than zero

implies that the system operates correctly. We demonstrate stability from the existence of the equilibrium with the Jacobian.

Theorem 2 *Let Assumption 2 hold and let a shift on consumption ΔP_i^L in each load node be given. Then system (15)–(17) is asymptotically stable at the equilibrium point if*

$$\begin{aligned} -1 - k_i\left(2\frac{\bar{V}_i}{R_{ii}} + \sum_{j\in\mathcal{N}_i}\frac{\bar{V}_i - \bar{V}_j}{R_{ij}}\right) < 0, \text{ for } i \in \mathcal{V}_G, \\ -1 - k_i\left(2\frac{\bar{V}_i}{R_{ii}} + \sum_{j\in\mathcal{N}_i}\frac{\bar{V}_i - \bar{V}_j}{R_{ij}} - 1\right) < 0, \text{ for } i \in \mathcal{V}_L. \end{aligned} \tag{18}$$

Proof Calculating the Jacobian of system (15)–(16) with respect to the states V_i and ΔP_i^L, yields the following $(n+l)\times(n+l)$ matrix:

$$J = \left[\begin{array}{c|c} \boldsymbol{J}^V & -k\tau_v^{-1} \\ \hline \mathbf{0}_{l\times n} & \begin{matrix}\mathbf{0}_{(n-l)\times l} \\ -\tau^{-1}\end{matrix} \end{array}\right], \tag{19}$$

where $\tau^{-1} = diag(\tau_i^{-1})$ is an $l\times l$ matrix, and J^V is the $n\times n$ matrix corresponding to the Jacobian of the open-loop voltage dynamics (5) with respect to the state vector V:

$$J^V = -\tau_v^{-1} - k\tau_v^{-1}\left([\bar{V}]G + [G\bar{V}]\right), \tag{20}$$

which is composed of diagonal elements

$$J_{ii}^V = -\frac{1}{\tau_{vi}} - 2\frac{k_i}{\tau_{vi}}\bar{V}_i g_{ii} - \frac{k_i}{\tau_{vi}}\sum_{j\in\mathcal{N}_i}\bar{V}_j g_{ij}, \tag{21}$$

and non-diagonal elements

$$J_{ij}^V = -\frac{k_i}{\tau_{vi}}\bar{V}_i g_{ij}. \tag{22}$$

To obtain the stability conditions, the eigenvalues of our linearised system J should be obtained. However, due to the size of J, the analytic calculation of the eigenvalues is a daunting task. Let us employ the Gershgorin disc theorem to approximate the position of such eigenvalues within the complex plane.

From Assumption 2, a disc $\boldsymbol{\Delta}_i$ can be defined for each row i in J. This will encircle the position of the eigenvalue λ_i. Such a disc is centred at $C_i = J_{ii}$ along the real axis with a radius $R_i = \sum_{j\in\mathcal{N}_i}|J_{ij}|$.

At the equilibrium point, for the ith voltage state of the system, its disc $\boldsymbol{\Delta}_i(C_i, R_i)$ is defined for non-load nodes as

$$\begin{aligned} \boldsymbol{\Delta}_i\Bigg(-\frac{1}{\tau_{vi}} - 2\frac{k_i}{\tau_{vi}}\bar{V}_i g_{ii} - \frac{k_i}{\tau_{vi}}\sum_{j\in\mathcal{N}_i}\bar{V}_j g_{ij}, \\ \sum_{j\neq i\in\mathcal{N}_i}\left|-\frac{k_i}{\tau_{vi}}\bar{V}_i g_{ij}\right|\Bigg), \text{ for } i \in \mathcal{V}_G, \end{aligned} \tag{23}$$

and if i is a load node as

$$\begin{aligned} \boldsymbol{\Delta}_i\Bigg(-\frac{1}{\tau_{vi}} - 2\frac{k_i}{\tau_{vi}}\bar{V}_i g_{ii} - \frac{k_i}{\tau_{vi}}\sum_{j\in\mathcal{N}_i}\bar{V}_j g_{ij}, \\ \sum_{j\in\mathcal{N}_i}\left|-\frac{k_i}{\tau_{vi}}\bar{V}_i g_{ij}\right| + \left|-\frac{k_i}{\tau_{vi}}\right|\Bigg), \text{ for } i \in \mathcal{V}_L. \end{aligned} \tag{24}$$

Figure 2 illustrates a possible configuration of such discs. Taking into account the properties of G mentioned in Section 2.3, the expression of $\boldsymbol{\Delta}_i(C_i, R_i)$ is simplified as follows:

$$\boldsymbol{\Delta}_i\left(-\frac{1}{\tau_{vi}} - 2\frac{k_i}{\tau_{vi}}\bar{V}_i g_{ii} - \frac{k_i}{\tau_{vi}}\sum_{j\in\mathcal{N}_i}\bar{V}_j g_{ij}, \frac{k_i}{\tau_{vi}}\bar{V}_i g_{ii} - \frac{k_i}{\tau_{vi}}\bar{V}_i g_i\right), \tag{25}$$

$$\begin{aligned} \boldsymbol{\Delta}_i\Bigg(-\frac{1}{\tau_{vi}} - 2\frac{k_i}{\tau_{vi}}\bar{V}_i g_{ii} - \frac{k_i}{\tau_{vi}}\sum_{j\in\mathcal{N}_i}\bar{V}_j g_{ij}, \\ \frac{k_i}{\tau_{vi}}\bar{V}_i g_{ii} - \frac{k_i}{\tau_{vi}}\bar{V}_i g_i + \frac{k_i}{\tau_{vi}}\Bigg), \text{if } i \in \mathcal{V}_L. \end{aligned} \tag{26}$$

For the system to be stable, the eigenvalues have to be positioned in the left-hand side of the complex plane, namely $\Re(\lambda_i) < 0$. To guarantee this, the entirety of Gershgorin discs should be in the left-hand-side of the complex plane, namely $C_i + R_i < 0$. This yields

$$\begin{aligned} -\frac{1}{\tau_{vi}} - \frac{k_i}{\tau_{vi}}\bar{V}_i g_{ii} - \frac{k_i}{\tau_{vi}}\sum_{j\in\mathcal{N}_i}\bar{V}_j g_{ij} - \frac{k_i}{\tau_{vi}}\bar{V}_i g_i < 0, \text{for } i \in \mathcal{V}_G, \\ -\frac{1}{\tau_{vi}} - \frac{k_i}{\tau_{vi}}\bar{V}_i g_{ii} - \frac{k_i}{\tau_{vi}}\sum_{j\in\mathcal{N}_i}\bar{V}_j g_{ij} - \frac{k_i}{\tau_{vi}}\bar{V}_i g_i + \frac{k_i}{\tau_{vi}} < 0, \text{for } i \in \mathcal{V}_L, \end{aligned}$$

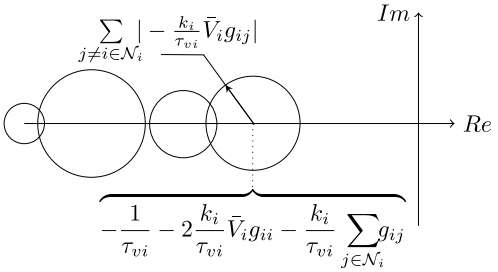

FIGURE 2 Gershgorin disc configuration example, the centre and radius for the ith disc of J

and simplifying the expressions above, the two conditions in (18) are obtained. Additionally, from J, the ΔP_i^L states yield l stable eigenvalues $\lambda_i = -1/\tau_i$, which is a straightforward result since the time constants are always positive. □

Remark 2 In the case where all of the node voltages have approximately the same value at the steady-state, that is, $\bar{V}_i \approx \bar{V}_j$, and the shunt conductances are small enough to be neglected $1/R_{ii} \approx 0$, condition (18) is simplified even further, yielding

$$k_i < 1, \tag{27}$$

which is a stronger assumption to the case studied. However, in practice $k_i = pV_i^*/P_i^{rated}\ \forall\, i$, where p is a percentage deviation of the node voltage that corresponds to 100% deviation of the real power, according to the droop control concept. The above result (27) yields the inequality $pV^* < P_i^{rated}$, which aligns with the low voltage network assumption.

4.5 | Implementing a bounded droop control architecture

It should be highlighted that in a real scenario, it is a requirement that the instantaneous node voltages remain within a given set, usually $V_i \in (V_i^* - \Delta V, V_i^* + \Delta V)\ \forall\, t \geq 0$, where ΔV is a deviation value of around 5%–10% from the rated voltage, namely $\Delta V = 0.05V^*$. Then, according to [24], we can use the bounded droop controller (BDC) to guarantee such outputs. This is based on the bounded integral control theory from [25]; a characteristic of this is that it still maintains the linear P-V controller approach [28] while generating a bounded output.

The above is achieved by introducing a second controller state V_q; hence the voltage dynamics for all the nodes take the following form:

$$\dot{V} = c\tau_v^{-1}((V^*\mathbf{1}_{n\times 1} - V) - k([V]GV - P^{set}))V_q^2, \tag{28}$$

$$\begin{aligned}\dot{V}_q = &-c\tau_v^{-1}\frac{V_q(V - V^*\mathbf{1}_{n\times 1})}{\Delta V^2}(V^*\mathbf{1}_{n\times 1} - V - k([V]GV - P^{set}))\\ &+ k^I\left(\frac{(V - V^*\mathbf{1}_{n\times 1})^2}{\Delta V^2} + V_q^2 - \mathbf{1}_{n\times 1}\right)V_q,\end{aligned} \tag{29}$$

where V_q is a vector with the same dimensions as V and $c = diag(c_i)$ and $k^I = diag(k_i^I)$ are matrices of positive constant gains for the integral control. The yielded state vector has the form $[V_1, \ldots, V_n, V_{q1}, \ldots, V_{qn}, \Delta P_1^L, \ldots, \Delta P_l^L]^T$. With the addition of V_q, it can be seen from (28)–(29) that the controller is composed of a non-linear double integrator structure, thus acting as an oscillator [24] and fulfiling the objective of emulating the dynamics of RMS voltage. Figure 3 illustrates the ways in which the values of the states V_i and V_{qi} start and remain in the upper part of the ellipse formed by the term $k^I\left(\frac{(V - V^*\mathbf{1}_{n\times 1})^2}{\Delta V^2} + V_q^2 - \mathbf{1}_{n\times 1}\right)$ in (29). The above has been previously demonstrated in detail in [25].

The closed-loop configuration of (28)–(29) for load nodes is now derived as

$$\begin{aligned}\dot{V}_i = \frac{c_i}{\tau_{vi}}\Big(&V_i^* - V_i - k_i\Big(V_i g_{ii} + V_i\sum_{j\in\mathcal{N}_i} V_j g_{ij}\\ &- P_i^{set} + \Delta P_i^L\Big)\Big)V_{qi}^2, \forall i \in \mathcal{V}_L,\end{aligned} \tag{30}$$

$$\begin{aligned}\dot{V}_{qi} = &-\frac{c_i}{\tau_{vi}}\frac{V_{qi}(V_i - V_i^*)}{\Delta V^2}\Big(V_i^* - V_i - k_i\Big(V_i g_{ii}\\ &+ V_i\sum_{j\in\mathcal{N}_i} V_j g_{ij} - P_i^{set} + \Delta P_i^L\Big)\Big)\\ &+ k_i^I\left(\frac{(V_i - V_i^*)^2}{\Delta V^2} + V_{qi}^2 - 1\right)V_{qi},\ \forall i \in \mathcal{V}_L.\end{aligned} \tag{31}$$

Similarly, for the generator nodes, the closed-loop dynamics are given as

$$\begin{aligned}\dot{V}_i = \frac{c_i}{\tau_{vi}}\Big(&V_i^* - V_i - k_i\Big(V_i g_{ii} + V_i\sum_{j\in\mathcal{N}_i} V_j g_{ij}\\ &- P_i^{set}\Big)\Big)V_{qi}^2, \forall i \in \mathcal{V}_G,\end{aligned} \tag{32}$$

$$\begin{aligned}\dot{V}_{qi} = &-\frac{c_i}{\tau_{vi}}\frac{V_{qi}(V_i - V_i^*)}{\Delta V^2}\Big(V_i^* - V_i - k_i\Big(V_i g_{ii}\\ &+ V_i\sum_{j\in\mathcal{N}_i} V_j g_{ij} - P_i^{set}\Big)\Big) + k_i^I\left(\frac{(V_i - V_i^*)^2}{\Delta V^2}\right.\\ &\left.+ V_{qi}^2 - 1\right)V_{qi},\ \forall i \in \mathcal{V}_G.\end{aligned} \tag{33}$$

The implementation of the BDC into our system dynamics also guarantees the existence of equilibrium points within selected bounds. With the introduction of the bounded voltage

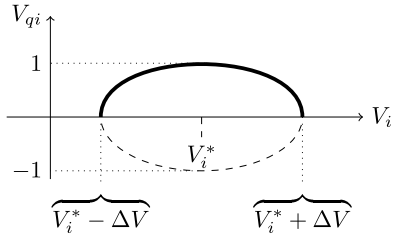

FIGURE 3 Bounded droop controller phase portrait example

dynamics, we can now relax Assumption 2 and present the result that follows:

Assumption 3 For constant inputs $D_i^{set}\ \forall i \in \mathcal{V}_L$ and $P_i^{set}\ \forall i \in \mathcal{V}_G$ with $P_{mg}^{set} = 0$, there exists an equilibrium point $[\bar{V}_1, \ldots, \bar{V}_n, \bar{V}_{q1}, \ldots, \bar{V}_{qn}, \Delta\bar{P}_1^L, \ldots, \Delta\bar{P}_l^L]^T$ for systems (15), (28)–(33), where $\Delta\bar{P}_i^L \in \mathbb{R}$, $\bar{V}_i \in \mathbb{R}_{>0}$, $\bar{V}_i \in (V^* - \Delta V, V^* + \Delta V)$ and $\bar{V}_{qi} \in (-1, 1)$.

This enables the stability conditions to be independent of the equilibrium point values $\bar{V}_i$ and to be dependent only on rated and tuned parameters:

Proposition 1 *Let Assumption 3 hold and let a shift on consumption ΔP_i^L in each load node be given; system (15), (30)–(33) is asymptotically stable at an equilibrium point if*

$$-1 - k_i\left(2\frac{V_i{}^* - \Delta V}{R_{ii}} - 2\Delta V\sum_{j\in\mathcal{N}_i}\frac{1}{R_{ij}}\right) < 0,\ \forall i \in \mathcal{V}. \tag{34}$$

Proof Denoting the V_q dynamics (31), (33) as $f(V, V_q, \Delta P^L)$ and calculating the Jacobian of systems (15), (30)–(33) with respect to the states V_i, V_{qi} and ΔP_i^L, we obtain the following $(2n + l) \times (2n + l)$ matrix:

$$J^{BDC} = \begin{bmatrix} \Phi J^V & \mathbf{0}_{n\times n} & -\Phi\kappa \\ \left.\frac{\partial f}{\partial V}\right|_{\bar{V},\Delta\bar{P}^L} & -\left[2k_i^I \bar{V}_{qi}{}^2\right] & \left.\frac{\partial f}{\partial \Delta P^L}\right|_{\bar{V},\Delta\bar{P}^L} \\ \mathbf{0}_{l\times n} & \mathbf{0}_{l\times n} & -\tau^{-1} \end{bmatrix}, \tag{35}$$

where κ is the $n \times l$ matrix $\kappa = \left[k\tau_v{}^{-1}, \mathbf{0}_{(n-l)\times l}\right]^T$ and Φ is a $n \times n$ matrix $\Phi = [c_i V_{qi}^2]$. For the stability conditions, the eigenvalues λ_i of linearised J^{BDC} are calculated. These are the roots of the polynomial yielded by the determinant

$$\left|\lambda I - J^{BDC}\right| = \left|\lambda I + \left[2k_i^I V_{qi}{}^2\right]\right|\left|\lambda I - \Phi J^V\right|\left|\lambda I + \tau^{-1}\right|. \tag{36}$$

Using the properties of block matrices, it is trivial to see that the $n + l$ eigenvalues yielded by both matrices $[2k_i^I V_{qi}{}^2]$ and τ^{-1} are negative and real due to the fact that all their values are positive. Thus, it remains only to find the eigenvalues of ΦJ^V. We can discard Φ and focus only on J^V since all values of $c_i V_{qi}^2$ are positive as well.

Similar to Section 4.3, computing the Gershgorin discs $\mathbf{\Delta}_i(C_i, R_i)$ of J^V with $C_i = J_{ii}^V$ and $R_i = \sum_{j\in\mathcal{N}_i}|J_{ij}^V|$, the following condition is obtained by shifting the entirety of disc $\mathbf{\Delta}_i$ to the left-hand side of the complex plane:

$$-\frac{1}{\tau_{vi}} - \frac{k_i}{\tau_{vi}}\bar{V}_i g_{ii} - \frac{k_i}{\tau_{vi}}\sum_{j\in\mathcal{N}_i}\bar{V}_j g_{ij} - \frac{k_i}{\tau_{vi}}\bar{V}_i g_i < 0,\ \forall i \in \mathcal{V}. \tag{37}$$

Simplifying the expression above, we can substitute $\bar{V}_i$ and $\bar{V}_j$ to the value that yields a disc closer to the origin. The worst case scenarios for such values are $\bar{V}_i = V_i^* - \Delta V$ and $\bar{V}_j = V_j^* + \Delta V$. Doing this we obtain the sufficient condition (34). □

Note that condition (34) can be easily checked since it does not require the calculation of the equilibrium point.

Now that the conditions for the stability of the integrated system have been explained, let us briefly focus on the ways in which the outcome of the game influences the physical system output.

After each play of the game, it can be demonstrated that the physical dynamics' equilibrium points depend directly on the game's output values. This can be corroborated as follows.

Remark 3 The steady-state expression for dynamics (15) of node $i \in \mathcal{VL}$ can be formulated as a function of the Stackelberg equilibrium parameters, namely

$$V_i{}^{ss} = f(\gamma, P_i^L, \alpha_{Ci}). \tag{38}$$

Once the consumers have decided their consumption and their demand has shifted, the dynamics (15) and (16) are considered to be at steady-state. From there the following expressions are obtained:

$$V_i{}^{ss} = k_i(P_i^{Lrated} - \Delta P_i^{Lss}) - k_i P_i + V_i{}^*, \tag{39}$$

$$\Delta P_i^{Lss} = D_i^{set}, \tag{40}$$

where P_i is shorthand for the static expression (2) at the equilibrium point. Substituting (13) into (40) yields

$$\Delta P_i^{Lss} = \frac{\alpha_{Ci}}{\gamma P_i^L} - P_i^{Lrated}. \tag{41}$$

This can be substituted into (39), resulting in the simplified expression

$$V_i^{ss} = k_i(2P_i^{Lrated} - \frac{\alpha_{Ci}}{\gamma P_i^L}) - k_i P_i + V_i^*, \tag{42}$$

which can be rewritten as the function in (38). It is worth mentioning that the steady state of the system will change value once the game has been played again. This is further exemplified in the numerical examples in the next section. The

above derivations can be performed similarly for the system subject to the bounded droop control presented in Section 4.5.

5 | SIMULATIONS

In this section we simulate three scenarios. In the first scenario we show how a single load behaves when subject to the incentive strategy. In the second, we show a configuration with two loads, where it is shown how consumer preferences can be modelled distinctly. Finally, in the third scenario we briefly demonstrate the scalability of our set-up by showing an instance with six loads and six generators. All examples are implemented using the closed-loop bounded droop control dynamics (15), (30)–(33) and the supplier and consumers involved are subject to the maximisation problem (11). The simulations are performed in Simulink.

In the first scenario the micro-grid consists of the following elements: one load (node 1), two generators (nodes 2 and 3), and the micro-grid is connected to the main grid (node 4). The parameters are selected as in Tables 1 and 2, where the droop coefficients are calculated in a standard fashion as $k_i = 0.05V_i^*/P_i^{rated}$ and $c_i = \pi\Delta V/0.1k_iP_i^{rated}$ for all nodes. The network topology is given by the conductances in G from (43). The cost function gains α_G and α_{mg} have been selected in a way that illustrates that it is more costly to use power from the main grid, resulting in higher incentive values when the main grid provides power. To further illustrate the price change, during the simulation we modify the power contributed by the supplier's generators; this is achieved by modifying the generators' set powers to the values as in Table 1. The initial value of the incentive is set to $\gamma = 0.036$ \$/W^2.

In all simulations, for example purposes and without loss of generality, we have selected the game to be played every $T_S = 60$s in which a new γ is calculated. The consumption ΔP_1^{set} is calculated at $T_C = 62$s, meaning that the incentive is known by the consumer 2 s after being announced.

$$G = \begin{bmatrix} 13.7221 & -5.0000 & -4.1667 & -4.5455 \\ -5.0000 & 14.1197 & -4.3478 & -4.7619 \\ -4.1667 & -4.3478 & 12.5245 & -4.0000 \\ -4.5455 & -4.7619 & -4.0000 & 13.3174 \end{bmatrix} \quad (43)$$

Figure 4 shows the node's power plots. It can be seen that there is an incentive change every time the generators shift their value. As a consequence of this, a shift in the load happens depending on how high the incentive is. In particular, if the incentive γ increases, the price increases and the consumer reduces its consumption (making it less negative in the plot). It can also be seen that a higher contribution by the main grid leads to a higher price and vice versa. Finally, the plots show

TABLE 2 Fixed parameters for simulations

c_i	τ_i	ΔV	V_i^*
31.4159	3 s	11 V	220 V

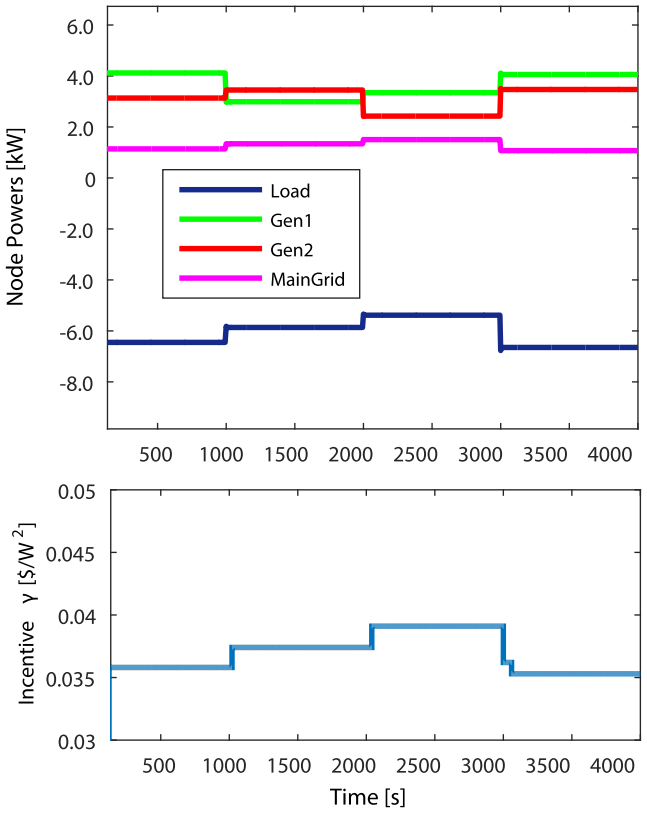

FIGURE 4 Simulation of a network connected to the main grid with one load and two varying generators

TABLE 1 First scenario parameters

	P^{set}	α_{Ci}	α_{Gi}	P^{rated}	k_i
Load 1	−6 kW	29×10^6 \$ $log(W)$	-	10 kW	0.0011
Generator 1	1.9 kW at $t = 0$ s 0.2 kW at $t = 1000$ s 2 kW at $t = 3000$ s	-	$11W^2$/\$	7 kW	0.0016
Generator 2	1.5 kW at $t = 0$ s 0.05 kW at $t = 2000$ s 2 kW at $t = 4000$ s	-		5 kW	0.0022
Main grid	0 kW	-	$2W^2$/\$	3 kW	0.0037

that given a change in the generators, both the incentive and the powers converge towards an equilibrium point. The voltage response stays within acceptable ranges and is mainly affected by the generator shifting as shown in Figure 5. It can be verified that the droop control is successful and there is no deviation larger than the 5% of the selected 220 V.

The second scenario consists of two loads (nodes 1 and 2), two generators (nodes 3 and 4), and the main grid (node 5). The power references are set as in Table 3. The cost and value function gains have been re-tuned. The latter have been set to show that the two consumers have different interests. Such values are selected due to the nature of their logarithmic value function, as in (10), and will depend on the kind of concave function selected as mentioned in Section 4.2. The topology is expanded from the previous with the conductances from (44). The rest of the parameters are left as in the previous simulation.

$$G = \begin{bmatrix} 17.5683 & -5.0000 & -4.1667 & -4.5455 & -3.8462 \\ -5.0000 & 17.8234 & -4.3478 & -4.7619 & -3.7037 \\ -4.1667 & -4.3478 & 16.0959 & -4.0000 & -3.5714 \\ -4.5455 & -4.7619 & -4.0000 & 16.7656 & -3.4483 \\ -3.8462 & -3.7037 & -3.5714 & -3.4483 & 14.5796 \end{bmatrix} \tag{44}$$

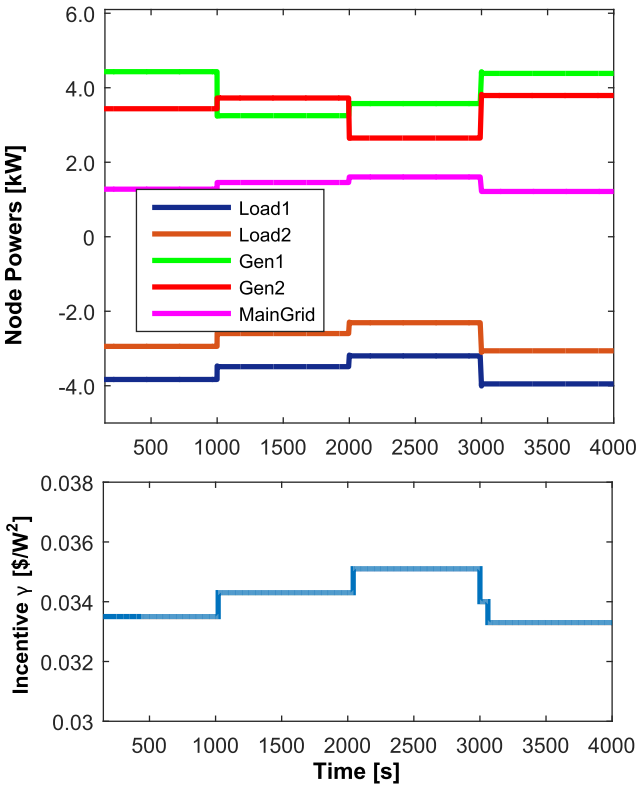

FIGURE 6 Simulation of a network connected to the main grid with two loads and two varying generators

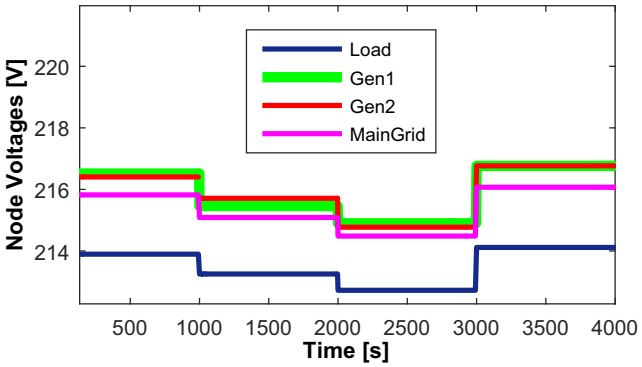

FIGURE 5 Voltage plots for the one load configuration

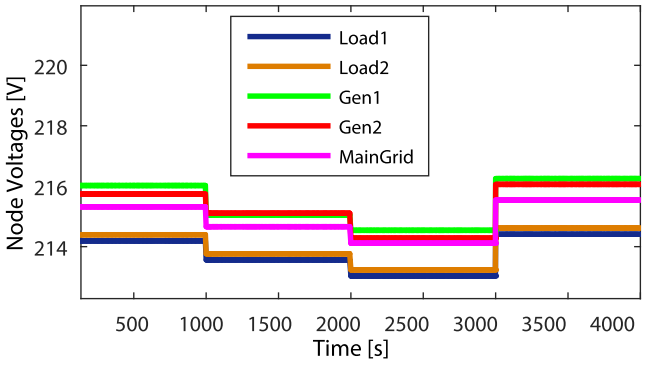

FIGURE 7 Voltage plots for the two load configuration

TABLE 3 Second scenario parameters

	P^{set}	α_{Ci}	α_{Gi}	P^{rated}	k_i
Load 1	−3.5 kW	29×10^6 \$ $/log(W)$	-	6 kW	0.0018
Load 2	−3.5 kW	20×10^6 \$ $/log(W)$	-	6 kW	0.0018
Generator 1	1.9 kW at $t = 0$ s 0.1 kW at $t = 1000$ s 2 kW at $t = 3000$ s	-	$9.5W^2/\$$	7 kW	0.0016
Generator 2	1.5 kW at $t = 0$ s 0.05 kW at $t = 2000$ s 2 kW at $t = 4000$ s	-		6 kW	0.0022
Main grid	0 kW	-	$7.5W^2/\$$	3 kW	0.0037

TABLE 4 Third scenario parameters

	P^{set}	α_{Ci}	α_{Gi}	P^{rated}	k_i
Load 1	−3.5 kW	29×10^6 \$ $/log(W)$	-	6 kW	0.0018
Load 2	−3.5 kW	20×10^6 \$ $/log(W)$	-	6 kW	0.0018
Load 3	−3.6 kW	18×10^6 \$ $/log(W)$	-	5.5 kW	0.0022
Load 4	−4.1 kW	10×10^6 \$ $/log(W)$	-	5 kW	0.0027
Load 5	−3.9 kW	7×10^6 \$ $/log(W)$	-	6 kW	0.0016
Load 6	−3.7kW	3×10^6 \$ $/log(W)$	-	5.7 kW	0.0014
Generator 1	1.9 kW at $t = 0$ s 0.1 kW at $t = 1000$ s 2 kW at $t = 3000$ s	-	$20W^2/\$$	7 kW	0.0016
Generator 2	1.5 kW at $t = 0$ s 0.05 kW at $t = 2000$ s 2 kW at $t = 3000$ s	-		5 kW	0.0022
Generator 3	1.9 kW at $t = 0$ s 0.1 kW at $t = 1000$ s 2 kW at $t = 3000$ s	-		5 kW	0.0022
Generator 4	1.5 kW at $t = 0$ s 0.05 kW at $t = 2000$ s 2 kW at $t = 3000$ s	-		6 kW	0.0018
Generator 5	1.9 kW at $t = 0$ s 0.1 kW at $t = 1000$ s 2 kW at $t = 3000$ s	-		8 kW	0.0014
Generator 6	1.5 kW at $t = 0$ s 0.05 kW at $t = 2000$ s 2 kW at $t = 3000$ s	-		7 kW	0.0016
Main grid	0 kW	-	$4.5W^2/\$$	3 kW	0.0037

Figure 6 shows the second power plots. As before, it can be seen that there is convergence towards different equilibrium points for different γ. The different consumer value gains α_{Ci} result in distinct steady states despite their equal rated and set consumption values, corroborating their influence on the steady-state value from (41). The voltage plots for the second scenario are shown in Figure 7. As expected, the inclusion of another load lowers the voltages overall. However, the 5% deviation from the set voltages is still satisfied by the droop controller.

The third scenario illustrates the power and consumption response of a micro-grid that consists of six interconnected loads (nodes 1 to 6), six generators (nodes 7–12), and is connected to the main grid (node 13). The parameters for the simulation are adopted as in Table 4 and its topology and respective conductances are shown in Figure 8. From Figure 9 it can be seen that, as in previous examples, the rationality of the consumers is captured as they react to the price accordingly. We should emphasise that the consumers have similar rated and set power values, and they shift to different values because we have selected a different α_{Ci} for each. To avoid repetition, we do not provide the voltage

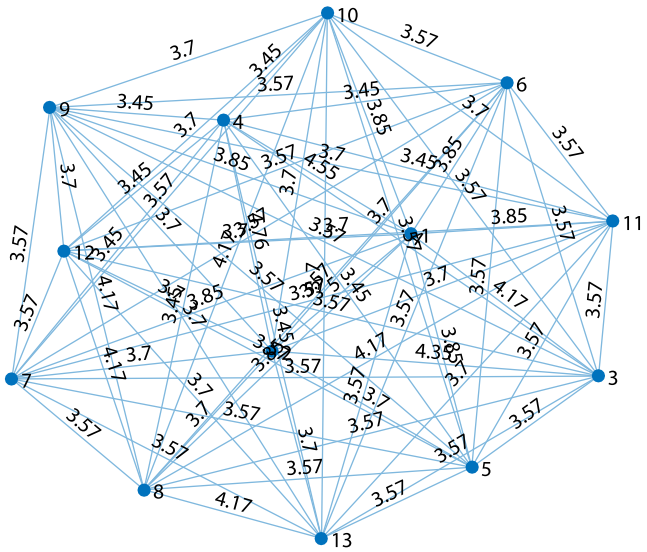

FIGURE 8 Graph topology corresponding to the third simulation scenario, where each edge represents the conductance between each micro-grid element

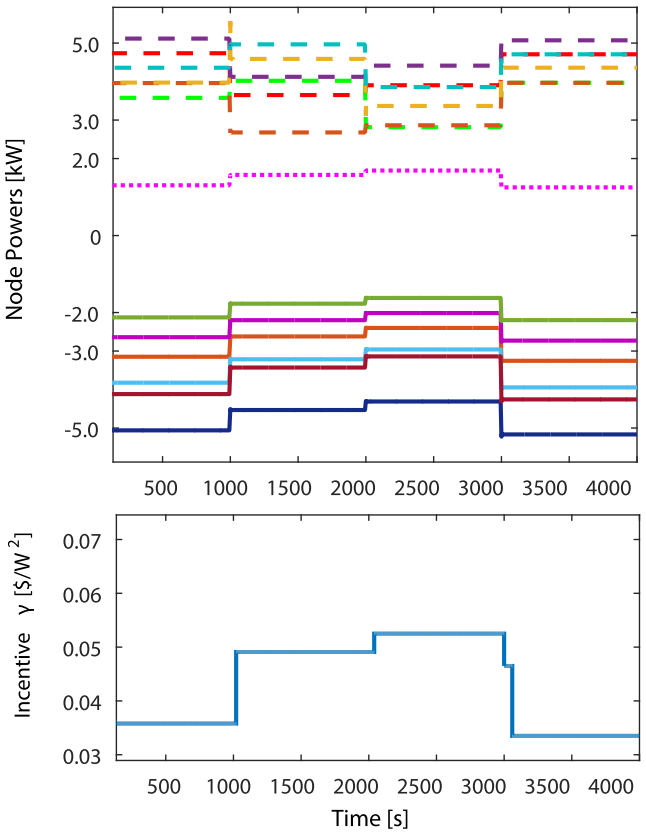

FIGURE 9 Simulation of a network connected to the main grid (dotted) with six loads (solid) and six varying generators (dashed)

response due to the similarity with the previous scenarios. Additionally, the system response remains stable, reaffirming both the feasibility and the scalability of our setup.

It is worth noting that in these simulations, the rational behaviour for both the supplier and the consumer has been captured: When the main grid contributes more power, its higher cost forces the supplier to increase the incentive which results in higher prices; in response, the consumer lowers its load to a point that brings it a better profit given the current price. The converse case that occurs when the contribution from the main grid is low, leading to a decrease of the price and an increase of the loads, is also captured at the latter part of the simulations. As a final note, the simulation results for the system without using the bounded droop control are very similar to the ones presented and are not shown here for the sake of brevity. However, it is easy to check that condition (18) holds based on the parameters used above.

6 | CONCLUSION

We have implemented a game-theoretical approach for online pricing on a low-voltage resistive micro-grid, bridging the gap between the market and physical components of the problem. We have proposed a game model that captures the rationality of the energy consumers. We have provided asymptotic stability conditions and shown how the parameters and functions can be adopted for the implementation of the online pricing mechanism. We have provided numerical examples that illustrate the ways in which the game and dynamics can be implemented, successfully capturing the rationality of the players involved together with the physical micro-grid, while also demonstrating stability at different equilibrium points. Future work will involve the inclusion of different functions for the incentive strategy, studying the bounds for the gains in both value and cost functions and the analytical conditions that lead to a consensus on price and demand and that ensure a non-oscillating response.

ACKNOWLEDGEMENT

Fernando Genis Mendoza is sponsored by Mexico's CONACyT, scholarship number: 440742. This work is supported by EPSRC (Grants Nos EP/S001107/1 and EP/S031863/1) and the Research Committee of the University of Patras via "C. CARATHEODORY" program (Grant 81359).

CONFLICT OF INTEREST

Fernando Genis Mendoza and Dario Bauso declare that they have no conflict of interest. George Konstantopoulos is an Associate Editor of IET Smart Grid.

PERMISSION TO REPRODUCE MATERIALS FROM OTHER SOURCES

None.

DATA AVAILABILITY STATEMENT

Data sharing not applicable to this article as no datasets were generated or analysed during the current study.

ORCID

Fernando Genis Mendoza https://orcid.org/0000-0001-7483-0654
George Konstantopoulos https://orcid.org/0000-0003-3339-6921
Dario Bauso https://orcid.org/0000-0001-9713-677X

REFERENCES

1. Genis Mendoza, F., Bauso, D., Konstantopoulos, G.: Online pricing via Stackelberg and incentive games in a micro-grid. In: 2019 18th European Control Conference, ECC 2019, pp. 3520–3525. IEEE (2019)
2. Roozbehani, M., Dahleh, M.A., Mitter, S.K.: Volatility of power grids under real-time pricing. IEEE Trans Power Syst. 27(4), 1926–1940 (2012)
3. Namerikawa, T., et al.: Real-time pricing mechanism for electricity market with built-in incentive for participation. IEEE Trans. Smart Grid. 6(6), 2714–2724 (2015)
4. Osborne, M.J.: A course in game theory. Comput. Math. Appl. 29(3), 115 (1995)
5. Ehtamo, H., Hämäläinen, R.P.: Incentive strategies and equilibria for dynamic games with delayed information. J Optim. Theor. Appl. 63(3), 355–369 (1989)
6. Tushar, W., et al.: Economics of electric vehicle charging: a game theoretic approach. IEEE Trans. Smart Grid. (2012)
7. Yoon, S.G., et al.: Stackelberg-game-based demand response for at-home electric vehicle charging. IEEE Trans. Veh. Technol. 65(6), 4172–4184 (2016)

8. Yu, M., Hong, S.H.: A real-time demand-response algorithm for smart grids: a Stackelberg game approach. IEEE Trans. Smart Grid. 7(2), 879–888 (2016)
9. Lee, J., et al.: Distributed energy trading in microgrids: a game-theoretic model and its equilibrium analysis. IEEE Trans. Ind. Electron. 62(6), 3524–3533 (2015)
10. Ma, K., et al.: Energy trading and pricing in microgrids with uncertain energy supply: a three-stage hierarchical game approach. Energies. 10(5) (2017)
11. Belgana, A., Rimal, B.P., Maier, M.: Open energy market strategies in microgrids: a Stackelberg game approach based on a hybrid multi-objective evolutionary algorithm. IEEE Trans. Smart Grid. 6(3), 1243–1252 (2015)
12. Azim, M.I., Hossain, M.J., Pota, H.R.: Design of a controller for active power sharing in a highly-resistive microgrid. IFAC-PapersOnLine. 48(30), 288–293 (2015)
13. Simpson-Porco, J.W., Dörfler, F., Bullo, F.: On resistive networks of constant power devices. IEEE Trans. Circuits Syst. II. 62(8), 811–815 (2015)
14. Chua, L.O., Desoer, C.A., Kuh, E.S.: Linear and Nonlinear Circuits. McGraw-Hill (1987)
15. Dörfler, F., Bullo, F.: Kron reduction of graphs with applications to electrical networks. IEEE Trans. Circuits Syst. I. 1–14 (2010)
16. Simpson-Porco, J.W., Dörfler, F., Bullo, F.: Voltage stabilization in microgrids via quadratic droop control. IEEE Trans. Automat. Contr. 62(3), 1239–1253 (2017)
17. Materassi, D., Roozbehani, M., Dahleh, M.A.: Equilibrium price distributions in energy markets with shiftable demand. In: 2012 IEEE 51st IEEE Conference on Decision and Control (CDC), pp. 3183–3188. IEEE. (2012)
18. Gouda, M.M., Danaher, S., Underwood, C.P.: Building thermal model reduction using nonlinear constrained optimization. Build. Environ. 37(12), 1255–1265 (2002)
19. Bediako, A., et al.: Future residential load profiles: scenario-based analysis of high penetration of heavy loads and distributed generation. Energy Build. 75 (2014)
20. Adamek, F.: Demand response and energy storage for a cost optimal residential energy supply with renewable generation, Thesis. Eidgenössische Techn. Hochschule Zürich. 1, 178 (2011)
21. Eksin, C., Delic, H., Ribeiro, A.: Demand response management in smart grids with heterogeneous consumer preferences. IEEE Trans. Smart Grid. 6(6), 3082–3094 (2015)
22. Vives, X.: Strategic supply function competition with private information. Econometrica. 79(6), 1919–1966 (2011)
23. Ghosh, A., Aggarwal, V., Wan, H.: Exchange of renewable energy among prosumers using Blockchain with dynamic pricing, arXiv Pre-prints (2018)
24. Konstantopoulos, G.C., et al.: Bounded droop controller for parallel operation of inverters. Automatica. 53, 320–328 (2015)
25. Konstantopoulos, G.C., et al.: Bounded integral control of input-to-state practically stable nonlinear systems to guarantee closed-loop stability. IEEE Trans. Automat. Contr. 61(12), 4196–4202 (2016)
26. Bauso, D., Giarré, L., Pesenti, R.: Non-linear protocols for optimal distributed consensus in networks of dynamic agents. Syst. Contr. Lett. 55(11), 918–928 (2006)
27. Zhong, Q.C.: Synchronized and democratized smart grids to underpin the third industrial revolution. IFAC-PapersOnLine. 50, 3592–3597 (2017)
28. Wang, Z., Lemmon, M.: Stability analysis of weak rural electrification microgrids with droop-controlled rotational and electronic distributed generators. In: 2015 IEEE Power Energy Society General Meeting, pp. 1–5. (2015)
29. Riaza, R.: A matrix pencil approach to the local stability analysis of nonlinear circuits. Int. J. Circ. Theor. Appl. 32(1), 23–46 (2004)
30. Schiffer, J., et al.: Conditions for stability of droop-controlled inverter-based microgrids. Automatica. 50(10), 2457–2469 (2014)
31. Simpson-Porco, J.W., Dörfler, F., Bullo, F.: Synchronization and power sharing for droop-controlled inverters in islanded microgrids. Automatica. 49(9), 2603–2611 (2013)

How to cite this article: Genis Mendoza, F., Konstantopoulos, G., Bauso, D.: Online pricing for demand-side management in a low-voltage resistive micro-grid via a Stackelberg game with incentive strategies. IET. Smart. Grid. 1–14 (2021). https://doi.org/10.1049/stg2.12053